Explicit lower bounds for Stokes eigenvalue problems by using nonconforming finite elements

Manting Xie[1] · **Hehu Xie**[2,3] · **Xuefeng Liu**[4]

Abstract An algorithm is proposed to give explicit lower bounds of the Stokes eigenvalues by utilizing two nonconforming finite element methods: Crouzeix–Raviart (CR) element and enriched Crouzeix–Raviart (ECR) element. Compared with the existing literatures which give lower eigenvalue bounds under the asymptotic condition that the mesh size is "small enough", the proposed algorithm in this paper drops the asymptotic condition and provide explicit lower bounds even for a rough mesh. Numerical experiments are also performed to validate the theoretical results.

This work is supported in part by National Science Foundations of China (NSFC 91730302, 11771434, 91330202, 11371026), Science Challenge Project (no. TZ2016002), the National Center for Mathematics and Interdisciplinary Science, CAS; X. Liu is supported by Japan Society for the Promotion of Science, Grand-in-Aid for Young Scientist (B) 26800090, Grant-in-Aid for Scientific Research (B) 16H03950.

✉ Xuefeng Liu
xfliu@math.sc.niigata-u.ac.jp

Manting Xie
mtxie@tju.edu.cn

Hehu Xie
hhxie@lsec.cc.ac.cn

1 Center for Applied Mathematics, Tianjin University, Tianjin 300072, China

2 LSEC, ICMSEC, Academy of Mathematics and Systems Science, Chinese Academy of Sciences, Beijing 100190, China

3 School of Mathematical Sciences, University of Chinese Academy of Sciences, Beijing 100049, China

4 Graduate School of Science and Technology, Niigata University, 8050 Ikarashi 2-no-cho, Nishi-ku, Niigata, Niigata 950-2181, Japan

Keywords Stokes eigenvalue problem · Eigenvalue bound · Crouzeix–Raviart element · Enriched Crouzeix–Raviart element · Explicit lower bound

Mathematics Subject Classification 65N30 · 65N25 · 65L15

1 Introduction

We are concerned with the explicit lower bounds of the eigenvalues for the Stokes eigenvalue problem by utilizing the finite element methods. The Stokes eigenvalue problem plays an important role in investigating the stabilities of the Navier–Stokes equations. For the aspect of numerical approach to Stokes eigenvalue problems, there have been many literatures in the history; see [3,8,11,12].

Recently, the verified computing has become a new approach to study nonlinear partial differential equations; see, e.g., [23–25,27]. Such an approach estimates all the error involved in the numerical computation and provides rigorous computation results, which can been even used for mathematical proof. For the eigenvalue problems of differential operators, rather than approximate eigenvalue evaluation with qualitative error estimation, *quantitative error estimation along with explicit bound for eigenvalues* are greatly wanted.

In this paper, we will consider the following Stokes eigenvalue problem and propose an algorithm to obtain explicit eigenvalue bounds: Find $(\lambda, \mathbf{u})$ s.t.

$$\begin{cases} -\Delta \mathbf{u} + \nabla p = \lambda \mathbf{u}, & \text{in } \Omega, \\ \nabla \cdot \mathbf{u} = 0, & \text{in } \Omega, \\ \mathbf{u} = 0, & \text{on } \partial\Omega, \\ \int_\Omega \mathbf{u}^2 \mathrm{d}\Omega = 1, \end{cases} \tag{1}$$

where $\Omega \subset \mathbb{R}^2$ denotes the computing domain with the Lipschiz boundary $\partial\Omega$; $\mathbf{u} = (u_1(x), u_2(x))^T$ is the velocity vector and $p = p(x)$ is the pressure. In addition, symbols Δ, ∇ and $\nabla\cdot$ denote the Laplacian, gradient and divergence operators, respectively.

So far, there have existed many results discussing the numerical methods for the eigenvalue problems. Chatelin [5], Babuška and Osborn [1,2] give an abstract convergence analysis for the eigenvalue problems by the finite element method (FEM). The error estimates for the mixed/hybrid FEM to the eigenvalue problems have been given by Osborn and Mercier et al. [22]. The a posteriori error estimators for the Stokes eigenvalue problem have been analyzed in [20] for conforming FEM and in [10] for nonconforming FEM. The asymptotic lower bounds for the elliptic and Stokes eigenvalues have been given in [14,15,17] and the two-sided bounds of the elliptic eigenvalues have already been discussed in [21].

The above mentioned methods only concern the *qualitative error estimation* for computable eigenvalues and it is difficult to obtain rigorous bound for the eigenvalue. For example, many nonconforming FEMs can provide lower eigenvalue bounds in the

asymptotic meaning, i.e., the mesh size is small enough. However, it is not an easy work to verify the condition of "small enough" for the mesh size.

Recently, Liu [19] proposes a novel framework to give explicit lower bounds for the eigenvalues, which drops the conditions on mesh size. The object of this paper is to apply Liu's framework to obtain explicit lower bounds for the Stokes eigenvalue problem (1). For this purpose, two nonconforming FEMs, i.e., Crouzeix–Raviart (CR) [7] element and enriched Crouzeix–Raviart (ECR) [9,18] element, will be considered along with explicit error estimation. As the main result summarized in Theorem 4, we show that

$$\lambda_i \geq \frac{\lambda_{i,h}^{(\ell)}}{1+(\alpha_l h)^2 \lambda_{i,h}^{(\ell)}} \ (\alpha_1 = 0.1893,\ \alpha_2 = 0.1490) \tag{2}$$

where λ_i denotes the ith eigenvalue of (1); $\lambda_{i,h}^{(\ell)}$ denotes the approximation to λ_i by applying CR element ($\ell = 1$) and ECR element ($\ell = 2$); h is the mesh size.

An outline of the paper goes as follows. In Sect. 2, we introduce the nonconforming FEMs along with explicit error estimation constants, for the Stokes eigenvalue problem (1). We present an explicit lower bounds of Stokes eigenvalues in Sect. 3. Some numerical examples are provided in Sect. 4 to validate our theoretical analysis. Some concluding remarks are given in the last section.

2 Preliminaries and nonconforming elements

In this section, we introduce the notation and the nonconforming FEMs to be used in discussing the Stokes eigenvalue problem (1).

2.1 Notation and weak form of Stokes eigenvalue problem

We shall use the standard notation for Sobolev spaces $W^{s,p}(\Omega)$ and their associated norms $\|\cdot\|_{s,p,\Omega}$ and seminorms $|\cdot|_{s,p,\Omega}$ (see, e.g., Chapter 1 of [4] and Chapter 1 of [6]). For $p = 2$, we denote $H^s(\Omega) = W^{s,2}(\Omega)$ and $H_0^1(\Omega) = \{v \in H^1(\Omega) : v|_{\partial\Omega} = 0\}$, where $v|_{\partial\Omega} = 0$ is in the sense of trace, $\|\cdot\|_{s,\Omega} = \|\cdot\|_{s,2,\Omega}$. In this paper, we set

$$\mathbf{V} = (H_0^1(\Omega))^2 \ \text{ and } \ Q = L_0^2(\Omega) = \left\{ q \in L^2(\Omega) : \int_\Omega q \mathrm{d}\Omega = 0 \right\}.$$

For the aim of finite element discretization, we define the corresponding weak form for (1) as follows: Find $(\lambda, \mathbf{u}, p) \in \mathbb{R} \times \mathbf{V} \times Q$ such that $r(\mathbf{u}, \mathbf{u}) = 1$ and

$$\begin{cases} a(\mathbf{u}, \mathbf{v}) - b(\mathbf{v}, p) = \lambda r(\mathbf{u}, \mathbf{v}), & \forall \mathbf{v} \in \mathbf{V}, \\ b(\mathbf{u}, q) = 0, & \forall q \in Q, \end{cases} \tag{3}$$

where

$$a(\mathbf{u},\mathbf{v}) := \int_\Omega \nabla\mathbf{u} : \nabla\mathbf{v}\mathrm{d}\Omega, \quad b(\mathbf{v},p) := \int_\Omega p\nabla\cdot\mathbf{v}\mathrm{d}\Omega,$$
$$r(\mathbf{u},\mathbf{v}) := \int_\Omega \mathbf{u}\cdot\mathbf{v}\mathrm{d}\Omega,$$

and $\nabla\mathbf{u} : \nabla\mathbf{v} = \sum_{i=1}^{2}\sum_{j=1}^{2}\frac{\partial u_i}{\partial x_j}\frac{\partial v_i}{\partial x_j}$.

We define

$$\mathbf{V}_0 := \{\mathbf{v}\in\mathbf{V} : b(\mathbf{v},q) = 0,\ \forall q\in Q\}. \tag{4}$$

Then the eigenvalue problem has an equivalent formulation as follows: Find $(\lambda,\mathbf{u})\in\mathbb{R}\times\mathbf{V}_0$ such that $r(\mathbf{u},\mathbf{u}) = 1$ and

$$a(\mathbf{u},\mathbf{v}) = \lambda r(\mathbf{u},\mathbf{v}),\quad \forall\mathbf{v}\in\mathbf{V}_0. \tag{5}$$

From Section 8 of [2], we know the eigenvalue problem (3) and (5) have the same eigenvalue series $\{\lambda_i\}_{i=1}^{\infty}$ such as

$$0 < \lambda_1 \le \cdots \le \lambda_i \le \cdots,\ \lim_{i\to\infty}\lambda_i = \infty,$$

and the corresponding eigenfunctions for (3)

$$(\mathbf{u}_1,p_1),\ldots,(\mathbf{u}_i,p_i),\ldots,$$

with $r(\mathbf{u}_i,\mathbf{u}_j) = \delta_{ij}$, where δ_{ij} is the Kronecker symbol.

Meanwhile, the following minimum–maximum and maximum–minimum principles hold:

$$\lambda_i = \frac{a(\mathbf{u}_i,\mathbf{u}_i)}{r(\mathbf{u}_i,\mathbf{u}_i)} = \min_{\substack{\mathbf{S}_i\subset\mathbf{V}_0\\ \dim(\mathbf{S}_i)=i}}\max_{\mathbf{v}\in\mathbf{S}_i}\frac{a(\mathbf{v},\mathbf{v})}{r(\mathbf{v},\mathbf{v})}$$
$$= \max_{\substack{\mathbf{X}\subset\mathbf{V}_0\\ \dim(\mathbf{X})\le i-1}}\min_{\mathbf{v}\in\mathbf{X}^\perp}\frac{a(\mathbf{v},\mathbf{v})}{r(\mathbf{v},\mathbf{v})}, \tag{6}$$

where $\mathbf{X}^\perp$ denotes the complementary space of $\mathbf{X}$ in $\mathbf{V}_0$ respect to the inner product $a(\cdot,\cdot)$.

2.2 Nonconforming finite element methods

In this subsection, we will introduce two kinds of nonconforming finite elements: CR [7] element and ECR [9,18] element. Throughout the paper, the index l is used to distinguish the terms related the two element: $\ell = 1$ for CR element; $\ell = 2$ for ECR element.

First, we introduce a regular triangular partition $\mathcal{T}_h$ to the domain Ω such that

$$\overline{\Omega} = \bigcup_{K \in \mathcal{T}_h} K.$$

The diameter of a cell $K \in \mathcal{T}_h$ is denoted by h_K and the mesh size h describes the maximum value of h_K among all K of $\mathcal{T}_h$. Denote the set of all interior edges of $\mathcal{T}_h$ as $\mathcal{E}_h$, the set of the edges on the boundary as $\mathcal{E}_{\partial\Omega}$ and $\mathcal{E} = \mathcal{E}_h \bigcup \mathcal{E}_{\partial\Omega}$.

The CR and ECR finite element spaces are defined as follows:

– CR element [7]

$$\mathcal{P}_1 = \text{span}\{1, x, y\}, \quad \mathbf{V}_h^{(1)} = (V_h^{(1)}(\Omega))^2,$$
$$Q_h = \{q \in L_0^2(\Omega) : q|_K \in \mathcal{P}_0, \forall K \in \mathcal{T}_h\},$$

where

$$V_h^1(\Omega) = \Big\{ v \in L^2(\Omega) : v|_K \in \mathcal{P}_1, \forall K \in \mathcal{T}_h; \int_e v|_{K_1} \mathrm{d}s = \int_e v|_{K_2} \mathrm{d}s, \forall e \in \partial K_1 \cap \partial K_2 \in \mathcal{E}_h; \int_e v \mathrm{d}s = 0 \text{ for } e \in \mathcal{E}_{\partial\Omega} \Big\}. \tag{7}$$

– ECR element [9,18]

$$E\mathcal{P}_1 = \text{span}\{1, x, y, x^2 + y^2\}, \quad \mathbf{V}_h^{(2)} = (V_h^{(2)}(\Omega))^2,$$
$$Q_h = \{q \in L_0^2(\Omega) : q|_K \in \mathcal{P}_0, \forall K \in \mathcal{T}_h\},$$

where

$$V_h^2(\Omega) = \Big\{ v \in L^2(\Omega) : v|_K \in E\mathcal{P}_1, \forall K \in \mathcal{T}_h; \int_e v|_{K_1} \mathrm{d}s = \int_e v|_{K_2} \mathrm{d}s, \forall e \in \partial K_1 \cap \partial K_2 \in \mathcal{E}_h; \int_e v \mathrm{d}s = 0 \text{ for } e \in \mathcal{E}_{\partial\Omega} \Big\}. \tag{8}$$

Due to the discontinuity of functions on edges, we know $\mathbf{V}_h^{(\ell)} \nsubseteq \mathbf{V}$, $\ell = 1, 2$.

Define the following bilinear forms for both CR and ECR finite element spaces, for all $\mathbf{u}_h, \mathbf{v}_h \in \mathbf{V}_h^{(\ell)} (\ell = 1, 2)$ and $q_h \in Q_h$,

$$a_h(\mathbf{u}_h, \mathbf{v}_h) := \sum_{K \in \mathcal{T}_h} \int_K \nabla \mathbf{u}_h : \nabla \mathbf{v}_h \mathrm{d}K, \quad b_h(\mathbf{v}_h, q_h) := \sum_{K \in \mathcal{T}_h} \int_K q_h \nabla \cdot \mathbf{v}_h \mathrm{d}K.$$

Corresponding to $\mathbf{V}_0$, define the subspace of $\mathbf{V}_h^{(\ell)} (\ell = 1, 2)$

$$\mathbf{V}_{0,h}^{(\ell)} = \{\mathbf{v}_h \in \mathbf{V}_h^{(\ell)} : b_h(\mathbf{v}_h, q_h) = 0, \ \forall q_h \in Q_h\}, \quad (\ell = 1, 2). \tag{9}$$

For $\mathbf{v} \in \mathbf{V} + \mathbf{V}_h^{(\ell)} (\ell = 1, 2)$, introduce the piecewise type norm and semi-norm:

$$\|\mathbf{v}\|_{1,h} = \left(\sum_{K \in \mathcal{T}_h} \sum_{i=1}^{2} \|v_i\|_{1,K}^2 \right)^{\frac{1}{2}}, \quad |\mathbf{v}|_{1,h} = \left(\sum_{K \in \mathcal{T}_h} \sum_{i=1}^{2} |v_i|_{1,K}^2 \right)^{\frac{1}{2}}.$$

In order to deduce the error estimates, we define the interpolation operators for CR and ECR elements as follows:

– For CR element, the interpolation operator $\Pi_h^1 : H^1(\Omega) \to V_h^1$ is defined by, for any $v \in H^1(\Omega)$

$$\int_e (v - \Pi_h^1 v) \mathrm{d}s = 0, \quad \forall e \in \mathcal{E}. \tag{10}$$

– For ECR element, the interpolation operator $\Pi_h^2 : H^1(\Omega) \to V_h^2$ is defined by, for any $v \in H^1(\Omega)$

$$\int_e (v - \Pi_h^2 v) \mathrm{d}s = 0, \quad \forall e \in \mathcal{E}, \tag{11}$$

$$\int_K (v - \Pi_h^2 v) \mathrm{d}K = 0, \quad \forall K \in \mathcal{T}_h. \tag{12}$$

Define interpolation operator $\mathbf{\Pi}_h^{(\ell)} : \mathbf{V} \to \mathbf{V}_h^{(\ell)}$ $(\ell = 1, 2)$ as follows:

$$\Pi_h^{(\ell)} \mathbf{v} := (\Pi_h^{(\ell)} v_1, \Pi_h^{(\ell)} v_2) \in \mathbf{V}_h^{(\ell)}, \quad \forall \mathbf{v} = (v_1, v_2) \in \mathbf{V}. \tag{13}$$

Proposition 1 *Interpolation operator $\mathbf{\Pi}_h^{(\ell)}$ $(\ell = 1, 2)$ has the following properties.*

1. $\mathbf{\Pi}_h^{(\ell)} \mathbf{u} \in \mathbf{V}_{0,h}^{(\ell)}$ *for all* $\mathbf{u} \in \mathbf{V}_0^{(\ell)}$.
2. $\mathbf{\Pi}_h^{(\ell)}$ *is an orthogonal projection that maps* $\mathbf{V}$ *to* $\mathbf{V}_h^{(\ell)}$*, i.e., for any* $\mathbf{u} \in \mathbf{V}$*,*

$$a_h(\mathbf{u} - \mathbf{\Pi}_h^{(\ell)} \mathbf{u}, \mathbf{v}_h) = 0, \quad \forall \mathbf{v}_h \in \mathbf{V}_h^{(\ell)}. \tag{14}$$

3. $\mathbf{\Pi}_h^{(\ell)}$ *is an orthogonal projection that maps* $\mathbf{V}_0$ *to* $\mathbf{V}_{0,h}$*, i.e., for any* $\mathbf{u} \in \mathbf{V}_0$*,*

$$a_h(\mathbf{u} - \mathbf{\Pi}_h^{(\ell)} \mathbf{u}, \mathbf{v}_h) = 0, \quad \forall \mathbf{v}_h \in \mathbf{V}_{0,h}^{(\ell)}. \tag{15}$$

Proof 1. From the definition of interpolation $\mathbf{\Pi}_h^{(\ell)}$, for any $q_h \in Q_h$, noticing that for all $K \in \mathcal{T}_h$, $\nabla(q_h|_K) = 0$, we have

$$\begin{aligned} b_h(\mathbf{\Pi}_h^{(\ell)} \mathbf{u}, q_h) &= \sum_{K \in \mathcal{T}_h} \int_K q_h \nabla \cdot (\mathbf{\Pi}_h^{(\ell)} \mathbf{u}) \mathrm{d}K = \sum_{K \in \mathcal{T}_h} \int_{\partial K} q_h \mathbf{n} \cdot \mathbf{\Pi}_h^{(\ell)} \mathbf{u} \mathrm{d}s \\ &= \sum_{K \in \mathcal{T}_h} \int_{\partial K} q_h \mathbf{n} \cdot \mathbf{u} \mathrm{d}s = \sum_{K \in \mathcal{T}_h} \int_K q_h \nabla \cdot \mathbf{u} \mathrm{d}K = b_h(\mathbf{u}, q_h), \end{aligned}$$

where $\mathbf{n}$ is the outer normal vector of ∂K.
Since $\mathbf{u} \in \mathbf{V}_0$, we have

$$b_h(\mathbf{\Pi}_h^{(\ell)}\mathbf{u}, q_h) = b_h(\mathbf{u}, q_h) = 0, \quad \forall q_h \in Q_h.$$

Thus, $\mathbf{\Pi}_h^{(\ell)}\mathbf{u} \in \mathbf{V}_{0,h}^{(\ell)}$.

2. The orthogonality of $\mathbf{\Pi}_h^{(\ell)}$ inherits from the one of $\Pi_h^{(\ell)}$. It is easy to check that for $u \in H^1(\Omega)$ (see, e.g., [18,21]),

$$\int_K \nabla(\Pi_h^{(\ell)}u - u) \cdot \nabla v_h \mathrm{d}K = 0, \quad \forall v_h \in V_h^{(\ell)}. \tag{16}$$

Thus, the proof for property 2 can be easily done by summation of equation (16) for each K of triangulation and each component of $\mathbf{u} \in \mathbf{V}$.

3. Property 3 is an analogous result of property 2.

Now, we state the following lemmas and theorems for the interpolation error estimation of $\mathbf{\Pi}_h^{(\ell)}$.

Lemma 1 [19] *For any $K \in \mathcal{T}_h$, let e_1, e_2, e_3 be the edges of K. The following inequality holds for all $\varphi \in V_e^1(K)$*

$$\|\varphi\|_{0,K} \leq \alpha_1 h_K |\varphi|_{1,K}, \tag{17}$$

where $V_e^1(K) = \left\{\varphi \in H^1(K) : \int_{e_i} \varphi \mathrm{d}s = 0,\ i = 1, 2, 3\right\}$ and $\alpha_1 = 0.1893$.

Based on Lemma 1, an interpolation error estimate for the interpolation operator $\mathbf{\Pi}_h^1$ is easy to obtain.

Theorem 1 *For any $\mathbf{u} \in (H^1(\Omega))^2$, the following inequality holds for the interpolation operator $\mathbf{\Pi}_h^1$ defined by* (13)

$$\|\mathbf{u} - \mathbf{\Pi}_h^1\mathbf{u}\|_0 \leq \alpha_1 h |\mathbf{u} - \mathbf{\Pi}_h^1\mathbf{u}|_{1,h}, \tag{18}$$

where h is the mesh size.

Remark 1 It is easy to see the inequality (18), as a raw estimation, also holds by replacing $\mathbf{\Pi}_h^1$ with $\mathbf{\Pi}_h^2$, i.e.,

$$\|\mathbf{u} - \mathbf{\Pi}_h^2\mathbf{u}\|_0 \leq \alpha_1 h |\mathbf{u} - \mathbf{\Pi}_h^2\mathbf{u}|_{1,h}. \tag{19}$$

2.3 The optimal constant of ECR interpolation operator

In this subsection, we derive the optimal constant for the ECR interpolation $\mathbf{\Pi}_h^2$. The main discussion is performed on just one triangle element K.

Given $K \in \mathcal{T}_h$ with the edges denoted by e_1, e_2, e_3, define a linear function space over domain K,

$$V_e^2(K) := \left\{ \varphi \in H^1(K) : \int_{e_i} \varphi \mathrm{d}s = 0,\ i = 1, 2, 3,\ \int_K \varphi \mathrm{d}K = 0 \right\},$$

and introduce the constant

$$C(K) := \sup_{w \in V_e^2(K)} \frac{\|w\|_0}{|w|_1}.$$

Noticing that $V_e^2(K) = \{v - \Pi_h^2 v \mid v \in H^1(K)\}$, we have

$$C(K) = \sup_{v \in H^1(K)} \frac{\|v - \Pi_h^2 v\|_0}{|v - \Pi_h^2 v|_1}.$$

The constant $C(K)$ is given by $C(K) = \bar{\lambda}_1^{-1/2}$ and $\bar{\lambda}_1$ is the first eigenvalue of the following eigenvalue problem: Find $(\bar{\lambda}, \bar{u}) \in \mathbb{R} \times V_e^2(K)$ such that

$$\int_K \nabla \bar{u} \cdot \nabla \bar{v} \mathrm{d}K = \bar{\lambda} \int_K \bar{u}\bar{v} \mathrm{d}K,\ \ \forall \bar{v} \in V_e^2(K). \tag{20}$$

To estimate $\bar{\lambda}_1$, we take a regular triangulation $\overline{\mathcal{T}}_h$ of K and introduce the enriched Crouzeix–Raviart FEM space $V_{e,h}^2(K)$ over $\overline{\mathcal{T}}_h$ to approximate $V_e^2(K)$. The member function v_h of $V_{e,h}^2(K)$ has the following properties,

(a) the restriction of v_h on each element is spanned by $\{1, x, y, x^2 + y^2\}$;
(b) $\int_e v_h|_{T_1} \mathrm{d}s = \int_e v_h|_{T_2} \mathrm{d}s$, in case e is the common edge shared by two elements T_1 and T_2 of $\overline{\mathcal{T}}_h$;
(c) $\int_{e_i} v_h \mathrm{d}s = 0,\ i = 1, 2, 3$;
(d) $\int_K v_h \mathrm{d}K = 0$.

The variational equation (20) is solved approximately in FEM space as follows: Find $(\bar{\lambda}_h, \bar{u}_h) \in \mathbb{R} \times V_{e,h}^2(K)$ such that

$$\sum_{T \in \overline{\mathcal{T}}_h} \int_T \nabla \bar{u}_h \cdot \nabla \bar{v}_h \mathrm{d}T = \bar{\lambda}_h \int_K \bar{u}_h \bar{v}_h \mathrm{d}K,\ \ \forall \bar{v}_h \in V_{e,h}^2(K). \tag{21}$$

From [19] (see also the quotation in §3.2) and estimation of $\mathbf{\Pi}_h^2$ in (19), we know that $\bar{\lambda}_1$ of (20) has a lower bound as follows,

$$\bar{\lambda}_1 \geq \frac{\bar{\lambda}_{1,h}}{1 + (0.1893h)^2 \bar{\lambda}_{1,h}},$$

where $\bar{\lambda}_{1,h}$ is the first eigenvalue of (21).

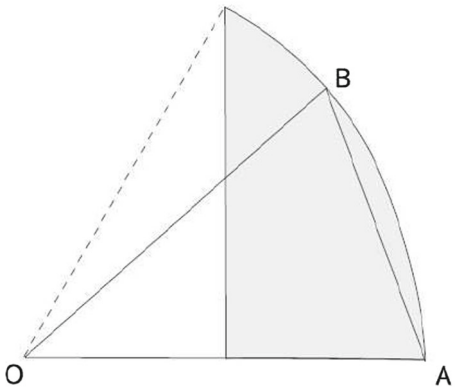

Fig. 1 Possible shapes of triangle OAB

In summary, for an element K, the constant $C(K)$ can be estimated by

$$C(K) \leq \left(\frac{\bar{\lambda}_{1,h}}{1 + (0.1893h)^2 \bar{\lambda}_{1,h}} \right)^{-1/2}. \tag{22}$$

Since we cannot evaluate $C(K)$ for all possible K. In the following, we show that the maximum of $C(K)$ can be estimated by considering several selected shapes of K.

As in Fig. 1, assume the three vertices of a triangle element K to be $O = (0, 0)$, $A = (1, 0)$ and $B = (a, b)$. Here vertex B is restricted by the conditions: $a \geq 1/2$, $b > 0$, $a^2 + b^2 \leq 1$. Notice that for any triangle element, it can be congruently transformed to a K considered here.

The following two lemmas about $C(K)$ can be obtained by applying the same arguments as in [19].

Lemma 2 (Theorem 4.1 of [19]) *For fixed x-coordinate of vertex B, the constant $C(K)$ is a monotonically increasing on the y-coordinate of vertex B. Therefore, the maximum value of $C(K)$ must be taken when B is on the arc such that $|\overline{OB}| = 1$, $\angle AOB \in (0, \pi/3]$.*

The following lemma is discussing the variation of $C(K)$ respect to the perturbation of B along the arc $r = 1$.

Lemma 3 (Theorem 4.2 of [19]) *For $0 < \theta < \pi/3$, let $\tilde{B} = (\cos(\theta + \tau), \sin(\theta + \tau))$ be a perturbation of $B = (\cos\theta, \sin\theta)$. Then, for $\tau < 0$ and $\theta + \tau > 0$, we have*

$$C(\tilde{K}) \leq \frac{\cos(\theta/2 + \tau/2)}{\cos(\theta/2)} C(K),$$

and for $\tau > 0$ and $\theta + \tau \leq \pi/3$, we have

$$C(\tilde{K}) \leq \frac{\sin(\theta/2 + \tau/2)}{\sin(\theta/2)} C(K),$$

where $\tilde{K} =$ triangle $OA\tilde{B}$.

To apply the Lemmas 2 and 3, we define θ_i by

$$\theta_i = \frac{\pi}{3} \times \begin{cases} i \times 0.02, & i = 1, \ldots, 48, \\ 0.95 + 0.05(1 - 0.8 \times 2^{48-i}), & i = 49, \ldots, 59, \\ 1, & i = 60. \end{cases} \tag{23}$$

Choose the perturbation τ_i as follows:

$$\tau_1 = \theta_1, \ \tau_i = \theta_i - \theta_{i-1}, \ i = 2, \ldots, 60.$$

Then we have $(0, \pi/3] = \cup_{i=1}^{60} (\theta_i - \tau_i, \theta_i]$.

We take two steps to bound all $C(K)$ for K with B located on the arc $r = 1, \ \theta = \angle AOB \in (0, \pi/3]$.

Step 1 For each θ_i defined in (23), choose K with $B = (\cos\theta_i, \sin\theta_i)$ and perform a uniform triangulation $\overline{\mathcal{T}}_h$ for K with mesh size being $h = 1/96$. In Fig. 2, we display a sample triangulation with $\theta_i = \pi/6$ and $h = 1/8$. Then we construct ECR finite element space $V_{e,h}^2$ based on $\overline{\mathcal{T}}_h$ and solve eigenvalue problem (21). A sharp upper bound of $C(K)$ is given by (22). In Fig. 3, we display the estimation of $C(K)$; the x-coordinate is taken as the angle size of $\angle AOB = \theta$. The estimation of $C(K)$ at each θ_i is denoted by a point.

Step 2 For each interval $(\theta_i - \tau_i, \theta_i]$, the upper bound of $C(K)$ is given by Lemma 3. In Fig. 3, the upper bound of $C(K)$ for each $\theta \in (\theta_i - \tau_i, \theta_i)$ is denoted by a short bar. The computation results show that for $\theta \in (0, \pi/3]$, $C(K)$ has an upper bound as $C(K) \leq 0.14899$. Also, a simple computation with conforming Lagrange FEM implies $C(K) > 0.14895$ for K being a unit regular triangle.

We draw the conclusion in the following theorem.

Theorem 2 *For any $K \in \mathcal{T}_h$ and any $\varphi \in V_e^2(K)$, the following inequality holds*

$$\|\varphi\|_{0,K} \leq \alpha_2 h_K |\varphi|_{1,K}, \tag{24}$$

where $\alpha_2 = 0.1490$.

The following theorem is a direct consequence of Theorem 2.

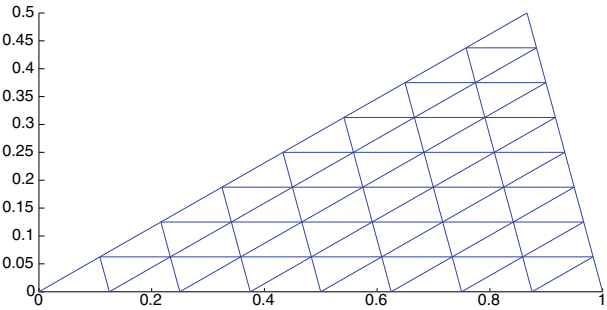

Fig. 2 Triangulation of K = triangle OAB with $\theta = \pi/6$ and $\bar{h} = 1/8$

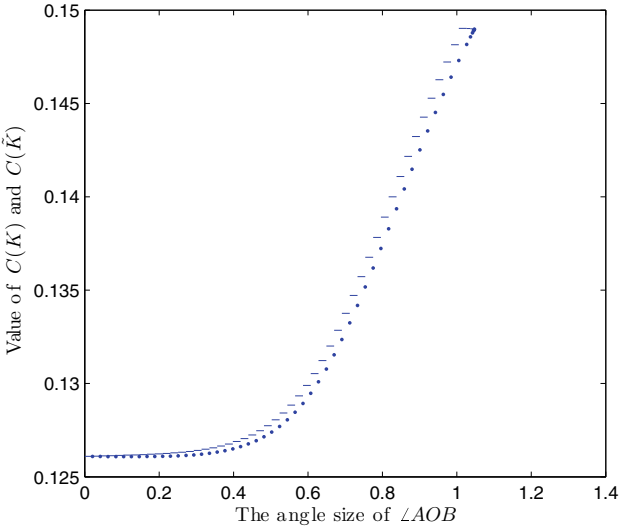

Fig. 3 Point-wise evaluation of $C(K)$ for each θ_i and the upper bound of $C(K)$ for $\theta \in (\theta_i - \tau_i, \theta_i)$

Theorem 3 *For any* $\mathbf{u} \in (H^1(\Omega))^2$, *the interpolation operator* $\mathbf{\Pi}_h^2$ *defined by* (13) *has the following estimate*

$$\|\mathbf{u} - \mathbf{\Pi}_h^2 \mathbf{u}\|_0 \leq \alpha_2 h |\mathbf{u} - \mathbf{\Pi}_h^2 \mathbf{u}|_{1,h}. \tag{25}$$

3 Nonconforming FEM and lower bound of Stokes eigenvalue

In this section, we show how to obtain explicit lower bounds for Stokes eigenvalues by using nonconforming FEMs.

3.1 Nonconforming FEM for Stokes eigenvalue problem

The Stokes eigenvalue problem (5) can be solved approximately by applying both CR and ECR nonconforming FEM: Find $(\lambda_h, \mathbf{u}_h, p_h) \in \mathbb{R} \times \mathbf{V}_h \times Q_h$ such that $r(\mathbf{u}_h, \mathbf{u}_h) = 1$ and

$$\begin{cases} a_h(\mathbf{u}_h, \mathbf{v}_h) - b_h(\mathbf{v}_h, p_h) = \lambda_h r(\mathbf{u}_h, \mathbf{v}_h), & \forall \mathbf{v}_h \in \mathbf{V}_h, \\ b_h(\mathbf{u}_h, q_h) = 0, & \forall q_h \in Q_h. \end{cases} \tag{26}$$

Here, the FEM space can be taken as $\mathbf{V}_h^{(1)}$ for EC element or $\mathbf{V}_h^{(2)}$ for ECR element. The eigenvalue problem has another kind formulation as follows: Find $(\lambda_h, \mathbf{u}_h) \in \mathbb{R} \times \mathbf{V}_{0,h}$ such that $r(\mathbf{u}_h, \mathbf{u}_h) = 1$ and

$$a_h(\mathbf{u}_h, \mathbf{v}_h) = \lambda_h r(\mathbf{u}_h, \mathbf{v}_h), \quad \forall \mathbf{v}_h \in \mathbf{V}_{0,h}, \tag{27}$$

where $\mathbf{V}_{0,h}$ is selected to be $\mathbf{V}_{0,h}^{(1)}$ or $\mathbf{V}_{0,h}^{(2)}$.

The discrete Stokes eigenvalue problem (26) and (27) have the same finite eigenvalue series $\{\lambda_{j,h}\}_{j=1}^{N}$

$$0 < \lambda_{1,h} \leq \cdots \leq \lambda_{i,h} \leq \cdots \leq \lambda_{N,h} < \infty,$$

and the corresponding eigenfunctions for (26)

$$(\mathbf{u}_{1,h}, p_{1,h}), \ldots, (\mathbf{u}_{i,h}, p_{i,h}), \ldots, (\mathbf{u}_{N,h}, p_{N,h}),$$

with $r(\mathbf{u}_{i,h}, \mathbf{u}_{j,h}) = \delta_{ij},\ 1 \leq i, j \leq N$, where $N = \dim \mathbf{V}_{0,h}$.

The inf-sup condition for the space $\mathbf{V}_h \times Q_h$ has been well investigated (cf. [7,18]):

$$\sup_{0 \neq \mathbf{v}_h \in \mathbf{V}_h} \frac{b_h(\mathbf{v}_h, q_h)}{\|\mathbf{v}_h\|_{1,h}} \geq \hat{C}\|q_h\|_0, \quad \forall q_h \in Q_h, \tag{28}$$

where $\hat{C} > 0$ is a constant independent of the mesh size h.

To confirm the convergence order of the lower bounds of eigenvalues to be explained in next sub-section, we recall the existing theoretical results. Assume that the eigenfunction $(\mathbf{u}_i, p_i)$ has the following regularity

$$\mathbf{u}_i \in (H^{1+\gamma}(\Omega))^2, \quad p_i \in H^{\gamma}(\Omega),$$

where γ depends on the shape of domain Ω ($\gamma = 1$ when Ω is convex). The following priori error estimates for approximate eigenpairs hold (see, e.g., [20]).

Lemma 4 [20, Theorem 2.1] *For any eigenpair approximation $(\lambda_{i,h}, \mathbf{u}_{i,h}, p_{i,h})$ of (27) ($i = 1, 2, \ldots, N$), there exists an exact eigenpair $(\lambda_i, \mathbf{u}_i, p_i)$ of (5) such that*

$$\|\mathbf{u}_i - \mathbf{u}_{i,h}\|_{1,h} + \|p_i - p_{i,h}\|_0 \leq Ch^{\gamma}(\|\mathbf{u}\|_{1+\gamma} + \|p\|_{\gamma}), \tag{29}$$

$$\|\mathbf{u}_i - \mathbf{u}_{i,h}\|_0 \leq Ch^{\gamma}\|\mathbf{u}_i - \mathbf{u}_{i,h}\|_{1,h}, \tag{30}$$

$$|\lambda_i - \lambda_{i,h}| \leq C\|\mathbf{u}_i - \mathbf{u}_{i,h}\|_{1,h}^2, \tag{31}$$

where C is a constant independent of mesh sizes h but dependent on the eigenvalue λ_i.

3.2 Lower bound of Stokes eigenvalue

In [19], a framework to bound eigenvalue for self-adjoint differential operators is proposed. In this section, we will verify the condition of the framework and apply it to obtain lower bound for Stokes eigenvalues.

Let Ω be a domain of $\mathbb{R}^m$ ($m = 1, 2, 3$). The framework proposed in [19] takes the following assumptions.

A1 V is a Hilbert space of real function on Ω with the inner product $M(\cdot, \cdot)$ and the corresponding norm $\|\cdot\|_M := \sqrt{M(\cdot, \cdot)}$.

A2 $N(\cdot,\cdot)$ is another inner product of V. The corresponding norm $\|\cdot\|_N := \sqrt{N(\cdot,\cdot)}$ is compact for V with respect to $\|\cdot\|_M$, i.e., every sequence in V which is bounded in $\|\cdot\|_M$ has a subsequence which is Cauchy in $\|\cdot\|_N$.
A3 V^h is a finite dimensional space of real function over Ω, $\mathrm{Dim}(V^h) = n$. Define $V(h) := V + V^h = \{v + v_h | v \in V, v_h \in V^h\}$.
A4 Bilinear forms $M_h(\cdot,\cdot)$ and $N_h(\cdot,\cdot)$ on $V(h)$ are extension of $M(\cdot,\cdot)$ and $N(\cdot,\cdot)$ to $V(h)$ such that
- $M_h(u, v) = M(u, v)$, $N_h(u, v) = N(u, v)$ for all $u, v \in V$.
- $M_h(\cdot,\cdot)$ and $N_h(\cdot,\cdot)$ are symmetric and positive definite on $V(h)$.

The assumption **A4** implies that $M_h(\cdot,\cdot)$ and $N_h(\cdot,\cdot)$ are also inner products of $V(h)$. For purpose of simplicity, the extended bilinear forms $M_h(\cdot,\cdot)$ and $N_h(\cdot,\cdot)$ are still denoted by $M(\cdot,\cdot)$ and $N(\cdot,\cdot)$ and the corresponding norms are denoted by $\|\cdot\|_M$ and $\|\cdot\|_N$, respectively.

Consider the eigenvalue problem defined in V and V^h:
(**P1**) Find $u \in V$ and $\lambda \in R$ such that,

$$M(u, v) = \lambda N(u, v) \quad \forall v \in V. \tag{32}$$

The eigenvalues are denoted by $0 < \lambda_1 \le \lambda_2 \le \ldots$
(**P2**) Find $u_h \in V^h$ and $\lambda_h \in R$ such that,

$$M(u_h, v_h) = \lambda_h N(u_h, v_h) \quad \forall v_h \in V^h. \tag{33}$$

The eigenvalues are denoted by $0 < \lambda_{h,1} \le \lambda_{h,2} \le \cdots \le \lambda_{h,n}$.

With the above assumption **A1**–**A4**, the lower eigenvalue bounds for (32) are given as follows.

Lemma 5 [19, Theorem 2.1] *Let $P_h : V(h) \to V^h$ be the projection with respect to inner product $M(\cdot,\cdot)$, i.e., for any $u \in V(h)$*

$$M(u - P_h u, v_h) = 0 \quad \forall v_h \in V^h. \tag{34}$$

Suppose the following error estimation holds for P_h: for any $u \in V$,

$$\|u - P_h u\|_N \le C_h \|u - P_h u\|_M. \tag{35}$$

Then, we have

$$\frac{\lambda_{h,i}}{1 + \lambda_{h,i} C_h^2} \le \lambda_i \quad (i = 1, 2, \ldots, n). \tag{36}$$

To apply the above theorem to obtain lower eigenvalue bounds for Stokes eigenvalue problem, we take the following settings.

$$V := \mathbf{V}_0 \text{ (see (4))}, \quad M(\cdot,\cdot) := a_h(\cdot,\cdot), \quad N(\cdot,\cdot) := r(\cdot,\cdot).$$

The function space V^h, projection P_h and constant C_h are taken as below:

$$\begin{cases} V^h := \mathbf{V}_{0,h}^{(1)}, & P_h := \mathbf{\Pi}_h^1, \quad C_h = \alpha_1 h \quad \text{for CR element;} \\ V^h := \mathbf{V}_{0,h}^{(2)}, & P_h := \mathbf{\Pi}_h^2, \quad C_h = \alpha_2 h \quad \text{for ECR element.} \end{cases}$$

Now, we reach the main result of this paper.

Theorem 4 *Let λ_i be the ith eigenvalue of the Stokes eigenvalue problem (5), and $\lambda_{i,h}^{(\ell)}$ ($\ell = 1, 2$) be the ith eigenvalue approximation of the discrete problem (27) by using CR element ($\ell = 1$) and ECR element ($\ell = 2$). Then the following explicit lower bound holds*

$$\underline{\lambda}_{i,h}^{(\ell)} \le \lambda_i, \quad (1 \le i \le dim(V_{0,h}^{\ell})) \tag{37}$$

where

$$\underline{\lambda}_{i,h}^{(1)} = \frac{\lambda_{i,h}^{(1)}}{1 + (0.1893h)^2 \lambda_{i,h}^{(1)}} \text{ and } \underline{\lambda}_{i,h}^{(2)} = \frac{\lambda_{i,h}^{(2)}}{1 + (0.1490h)^2 \lambda_{i,h}^{(2)}}. \tag{38}$$

Corollary 1 *The lower bounds $\underline{\lambda}_{i,h}^{(\ell)}$ ($\ell = 1, 2$) defined by (38) has the following error estimate*

$$\lambda_i - \underline{\lambda}_{i,h}^{(\ell)} \le \tilde{C} h^{2\gamma}, \tag{39}$$

where $\tilde{C}$ is a constant independent of mesh sizes h but dependent on the eigenvalue λ_i.

Proof According to Lemma 4 and Theorem 4, for $\ell = 1, 2$, we have

$$\begin{aligned} \lambda_i - \underline{\lambda}_{i,h}^{(\ell)} &\le |\lambda_i - \lambda_{i,h}^{(\ell)}| + |\lambda_{i,h}^{(\ell)} - \underline{\lambda}_{i,h}^{(\ell)}| \\ &\le C h^{2\gamma} (\|\mathbf{u}\|_{1+\gamma} + \|p\|_{\gamma})^2 + \left| \lambda_{i,h}^{(\ell)} - \frac{\lambda_{i,h}^{(\ell)}}{1 + (\alpha_\ell h)^2 \lambda_{i,h}^{(\ell)}} \right| \\ &\le \left(C (\|\mathbf{u}\|_{1+\gamma} + \|p\|_{\gamma})^2 + {\alpha_\ell}^2 \frac{(\lambda_{i,h}^{(\ell)})^2}{1 + (\alpha_\ell h)^2 \lambda_{i,h}^{(\ell)}} \right) h^{2\gamma} \\ &\le \tilde{C} h^{2\gamma}. \end{aligned}$$

4 Numerical results

In this section, we provide two numerical examples to demonstrate the efficiency of the proposed lower eigenvalue bounds (37) and confirm the convergence order as given in (39).

The lower bound in formula (37) holds for elements of arbitrary shapes. Since we adopt the uniform mesh with only isosceles triangle elements in the following FEM computation (see a sample element in Fig. 4), a better estimation for the interpolation error in Theorems 1 and 3 is possible. By adopting the method in Sect. 2.3, we have

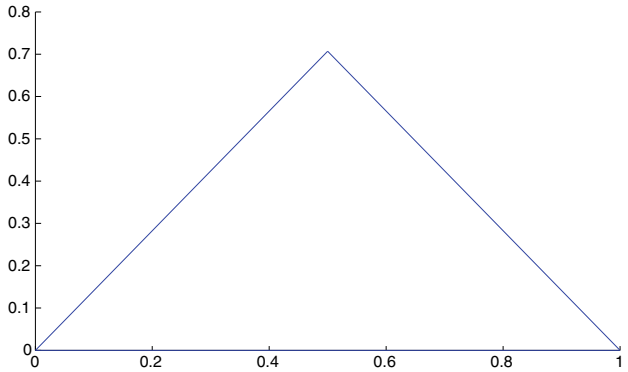

Fig. 4 Isosceles right triangle element K with $h_K = 1$

a sharper bound for the interpolation constants and the following interpolation error estimation is obtained

$$\|\mathbf{w} - \mathbf{\Pi}_h^{(\ell)}\mathbf{w}\|_0 \leq \tilde{\alpha}_\ell h |\mathbf{w} - \mathbf{\Pi}_h^{(\ell)}\mathbf{w}|_{1,h} \quad \forall \mathbf{w} \in (H^1(\Omega))^2, \tag{40}$$

where

$$\tilde{\alpha}_1 = 0.1761, \quad \tilde{\alpha}_2 = 0.1349.$$

We will apply the formula (37) in the following computing with α_ℓ replaced by $\tilde{\alpha}_\ell$ ($\ell = 1, 2$).

Example 1 In the first example, we solve the Stokes eigenvalue problem (5) with the CR element and ECR element on the unit domain $\Omega = (0, 1) \times (0, 1)$.

An uniform mesh is adopted for FEM computation. In Fig. 5, we display an initial triangulation of unit square $(0, 1) \times (0, 1)$ with the subdivision number $n = 2$ and mesh size $h = \sqrt{2}/2$. Then using the regular refinement (connecting three midpoints on the three edges for each element), we obtain a nested sequence of meshes with the subdivision number $n = 4, 8, \ldots, 128$ and mesh size $h = \sqrt{2}/4, \sqrt{2}/8, \ldots, \sqrt{2}/128$, as is shown in Fig. 5.

Since the exact eigenvalues of Stokes eigenvalue problem (5) are unknown, we use the extrapolation method (cf. Chapter 3, [13]) to obtain high-precision approximations, denoted by $\tilde{\lambda}_i$, for the exact eigenvalues. Such high-precision approximations are regarded as the "exact" value of eigenvalues in investigating the convergence order.

Once approximate eigenvalues are obtained by using the CR element and ECR element, we use the formula (38) to produce the explicit lower bounds for exact eigenvalues. Tables 1 and 2 shows the numerical results for the first 6 eigenvalues. From Tables 1 and 2, we see that $\underline{\lambda}_{i,h}^{(\ell)}$ ($\ell = 1, 2$) provide lower bounds of the exact eigenvalues λ_i ($i = 1, \ldots, 6$). Figure 6 presents the error estimates of $\underline{\lambda}_{1,h}^{(\ell)}, \ldots, \underline{\lambda}_{6,h}^{(\ell)}$ ($\ell = 1, 2$) which shows that the eigenvalue approximation $\underline{\lambda}_{i,h}^{(\ell)}(\ell = 1, 2)$ has the optimal second order convergence rate.

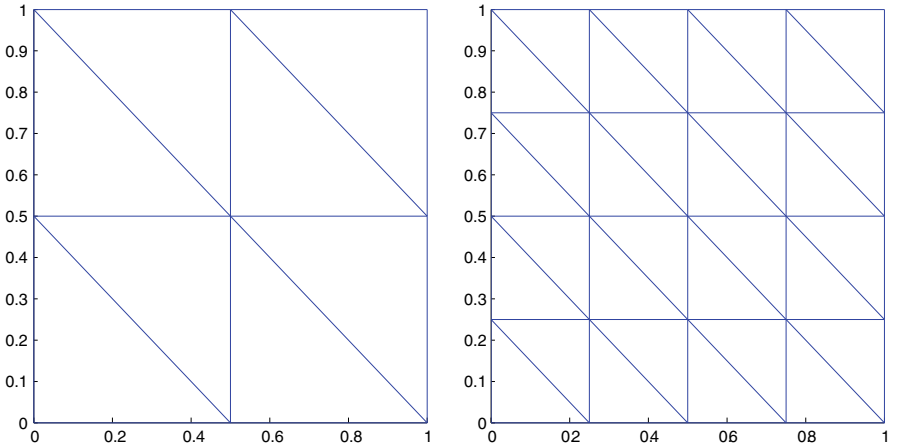

Fig. 5 The initial triangulation with $n = 2$ and a nested mesh with $n = 4$

Table 1 Numerical results of the CR element (square domain)

n	$\underline{\lambda}_{1,h}^{(1)}$	$\underline{\lambda}_{2,h}^{(1)}$	$\underline{\lambda}_{3,h}^{(1)}$	$\underline{\lambda}_{4,h}^{(1)}$	$\underline{\lambda}_{5,h}^{(1)}$	$\underline{\lambda}_{6,h}^{(1)}$
2	20.6752	20.6752	23.9345	24.0689	27.5186	38.5768
4	39.1567	48.5983	52.4052	62.5675	64.3435	67.4304
8	48.2522	77.4791	78.4128	104.4749	115.3565	130.4061
16	51.2334	88.1092	88.3322	121.3679	142.9868	156.5350
32	52.0595	91.0916	91.1478	126.4196	151.2339	164.2943
64	52.2728	91.8641	91.8783	127.7563	153.3954	166.3377
128	52.3267	92.0592	92.0627	128.0959	153.9425	166.8558
$\tilde{\lambda}_i$	52.3447	92.1244	92.1244	128.2095	154.1254	167.0291

Table 2 Numerical results of the ECR element (square domain)

n	$\underline{\lambda}_{1,h}^{(2)}$	$\underline{\lambda}_{2,h}^{(2)}$	$\underline{\lambda}_{3,h}^{(2)}$	$\underline{\lambda}_{4,h}^{(2)}$	$\underline{\lambda}_{5,h}^{(2)}$	$\underline{\lambda}_{6,h}^{(2)}$
2	21.3389	21.6893	24.7780	24.7855	28.5041	42.2255
4	39.2354	48.8589	53.1444	63.7816	65.2758	69.4798
8	48.2015	77.3689	78.3737	104.3997	115.4010	130.5313
16	51.2133	88.0513	88.2801	121.2694	142.8627	156.3912
32	52.0539	91.0747	91.1313	126.3877	151.1892	164.2419
64	52.2714	91.8597	91.8739	127.7479	153.3833	166.3234
128	52.3263	92.0581	92.0616	128.0937	153.9394	166.8521
$\tilde{\lambda}_i$	52.3447	92.1244	92.1244	128.2095	154.1254	167.0291

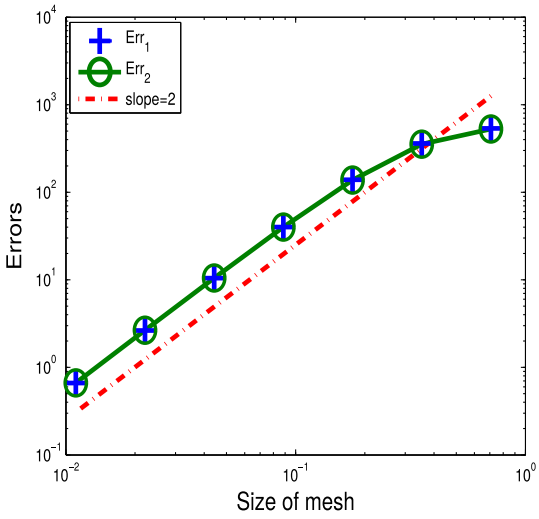

Fig. 6 The errors for the eigenvalue approximations $\underline{\lambda}_{i,h}^{(\ell)}$ on the unit square by the CR and ECR elements, where $\mathrm{Err}_1 = \sum_{i=1}^{6}(\tilde{\lambda}_i - \underline{\lambda}_{i,h}^{(1)})$ and $\mathrm{Err}_2 = \sum_{i=1}^{6}(\tilde{\lambda}_i - \underline{\lambda}_{i,h}^{(2)})$

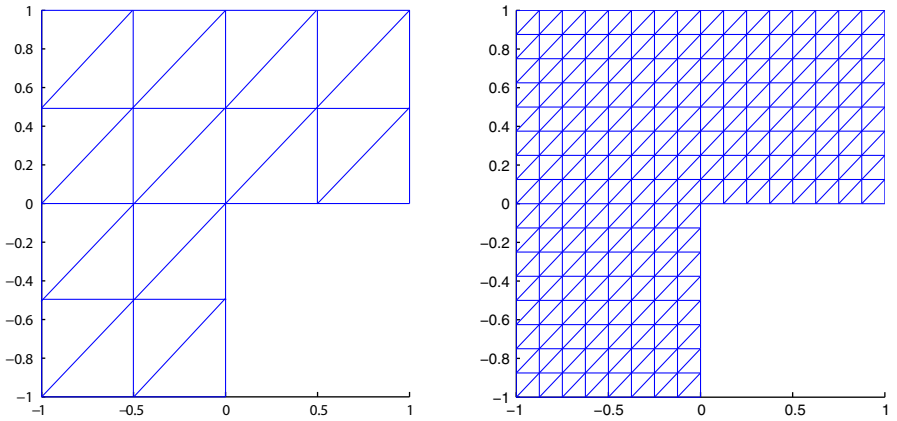

Fig. 7 The triangulations for the L-shaped domain ($n = 2$ and $n = 8$)

Example 2 In this example, we solve the Stokes eigenvalue problem (5) with the CR element and ECR element on the L-shape domain $\Omega = (-1, 1) \times (-1, 1)/[0, 1) \times (-1, 0]$.

Figure 7 shows the initial triangulation with the mesh subdivision number $n = 2$. By using the same refinement in Example 1, we obtain a nested sequence meshes with the mesh subdivision number $n = 4, 8, \ldots, 128$ such as in Fig. 7.

Using the same method in Example 1, we obtain high-precision approximations for the first 5 exact eigenvalues. From the numerical results in Tables 3 and 4, we see that the formula (37) gives lower bounds for the first 5 eigenvalues even the domain is not convex, in which case, the eigenfunction may has singularities around the reentrant corner.

Due to the singularities of eigenfunctions, the convergence order for both the eigenvalue approximations obtained by the CR and ECR methods and the obtained explicit

Table 3 Numerical results of the CR element (the L-shaped domain)

n	$\underline{\lambda}_{1,h}^{(1)}$	$\underline{\lambda}_{2,h}^{(1)}$	$\underline{\lambda}_{3,h}^{(1)}$	$\underline{\lambda}_{4,h}^{(1)}$	$\underline{\lambda}_{5,h}^{(1)}$
2	14.4695	14.7928	16.7622	18.7119	20.0988
4	24.5191	27.1142	31.7683	36.1125	39.3904
8	29.3292	33.8631	38.9161	45.0319	50.1740
16	31.1295	36.1243	41.1275	47.9096	53.8933
32	31.7564	36.7728	41.7249	48.7053	54.9773
64	31.9817	36.9512	41.8813	48.9125	55.2817
128	32.0685	36.9999	41.9229	48.9655	55.3707
$\tilde{\lambda}_i$	32.1397	37.0185	41.9404	48.9836	55.4184

Table 4 Numerical results of the ECR element (the L-shaped domain)

n	$\underline{\lambda}_{1,h}^{(2)}$	$\underline{\lambda}_{2,h}^{(2)}$	$\underline{\lambda}_{3,h}^{(2)}$	$\underline{\lambda}_{4,h}^{(2)}$	$\underline{\lambda}_{5,h}^{(2)}$
2	14.6024	15.0780	17.0872	19.1793	20.6885
4	24.4854	27.1196	31.7749	36.1692	39.4366
8	29.3046	33.8348	38.8798	44.9883	50.1138
16	31.1217	36.1141	41.1143	47.8921	53.8707
32	31.7543	36.7700	41.7213	48.7004	54.9710
64	31.9812	36.9505	41.8804	48.9113	55.2802
128	32.0684	36.9997	41.9226	48.9651	55.3703
$\tilde{\lambda}_i$	32.1397	37.0185	41.9404	48.9836	55.4184

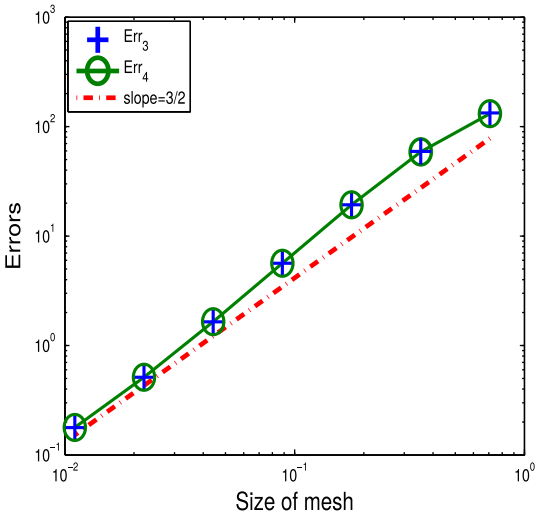

Fig. 8 The errors for the eigenvalue approximations $\underline{\lambda}_{i,h}^{(\ell)}$ on the L-shape domain by the CR and ECR elements, where $\mathrm{Err}_3 = \sum_{i=1}^{5}(\tilde{\lambda}_i - \underline{\lambda}_{i,h}^{(1)})$ and $\mathrm{Err}_4 = \sum_{i=1}^{5}(\tilde{\lambda}_i - \underline{\lambda}_{i,h}^{(2)})$

lower bound is less than 2, as is confirmed in Fig. 8 where numerical errors of $\underline{\lambda}_{1,h}^{(\ell)}, \ldots, \underline{\lambda}_{6,h}^{(\ell)}$ $(\ell = 1, 2)$ are displayed. We see that the eigenvalue approximation $\underline{\lambda}_{i,h}^{(\ell)}(\ell = 1, 2)$ has the optimal convergence rate as 2γ $(\gamma = 3/4)$.

5 Concluding remarks

In this paper, we give an explicit upper bound for constant $C(K)$ in ECR interpolation error estimation. Then by using the concrete value of $C(K)$, we provide an explicit lower bound for the exact Stokes eigenvalues by the CR and ECR elements. As the main feature of the proposed algorithm, *the lower eigenvalue bounds in* (37) *holds even for very rough mesh* (see the computation with subdivision number as $n = 2$). Also, such a lower bound has the optimal convergence order when mesh size tends to zero.

We would like to say the results and methods in this paper can be extended to the nonconforming FEMs $\mathrm{Q}_1^{\mathrm{rot}}$ [26] and $\mathrm{EQ}_1^{\mathrm{rot}}$ [16] since the framework in Sect. 3.2 can be easily verified.

References

1. Babuška, I., Osborn, J.E.: Finite element-Galerkin approximation of the eigenvalues and eigenvectors of selfadjoint problems. Math. Comput. **52**, 275–297 (1989)
2. Babuška, I., Osborn, J.: Eigenvalue problems. In: Lions, P.G., Ciarlet, P.G. (eds.) Handbook of Numerical Analysis, Vol. II, Finite Element Methods (Part 1), pp. 641–787. North-Holland, Amsterdam (1991)
3. Batcho, P., Karniadakis, G.: Generalized Stokes eigenfunctions: a new trial basis for the solution of the incompressible Navier–Stokes equations. J. Comput. Phys. **115**, 121–146 (1994)
4. Brenner, S., Scott, L.: The Mathematical Theory of Finite Element Methods. Springer, New York (1994)
5. Chatelin, F.: Spectral Approximation of Linear Operators. Academic Press Inc, New York (1983)
6. Ciarlet, P.G.: The Finite Element Method for Elliptic Problems. North-Holland, Amsterdam (1978)
7. Crouzeix, M., Raviart, P.: Conforming and nonconforming finite element for solving the stationary Stokes equations. RAIRO Anal. Numer. **3**, 33–75 (1973)
8. Fabes, E., Kenig, C., Verchota, G.: The Dirichlet problem for the Stokes system on Lipschitz domains. Duke Math. J. **57**, 769–793 (1998)
9. Hu, J., Huang, Y., Lin, Q.: The lower bounds for eigenvalues of elliptic operators by nonconforming finite element methods. J. Sci. Comput. **61**(1), 196–221 (2014)
10. Jia, S., Luo, F., Xie, H.: A posterior error analysis for the nonconforming discretization of Stokes eigenvalue problem. Acta Math. Sinica (Engl. Ser.) **30**(6), 949–967 (2014)
11. Labrosse, G., Leriche, E., Lallemand, P.: Stokes eigenmodes in cubic domain: their symmetry properties. Theor. Comput. Fluid Dyn. **28**(3), 335–356 (2014)
12. Leriche, E., Labrosse, G.: Stokes eigenmodes in square domain and the stream function–vorticity correlation. J. Comput. Phys. **200**, 489–511 (2004)
13. Lin, Q., Lin, J.: Finite Element Methods: Accuracy and Improvement. China Sci. Press, Beijing (2006)
14. Lin, Q., Luo, F., Xie, H.: A multilevel correction method for Stokes eigenvalue problems and its applications. Math. Methods Appl. Sci. **38**, 4540–4554 (2015)
15. Lin, Q., Luo, F., Xie, H.: A posterior error estimator and lower bound of a nonconforming finite element method. J. Comput. Appl. Math. **265**, 243–254 (2014)
16. Lin, Q., Tobiska, L., Zhou, A.: On the superconvergence of nonconforming low order finite elements applied to the Poisson equation. IMA J. Numer. Anal. **25**, 160–181 (2005)
17. Lin, Q., Xie, H.: The asymptotic lower bounds of eigenvalue problems by nonconforming finite element methods. Math. Pract. Theory (in Chinese) **42**(11), 219–226 (2012)
18. Lin, Q., Xie, H., Luo, F., Li, Y., Yang, Y.: Stokes eigenvalue approximation from below with nonconforming mixed finite element methods. Math. Pract. Theory (in Chinese) **19**, 157–168 (2010)
19. Liu, X.: A framework of verified eigenvalue bounds for self-adjoint differential operators. Appl. Math. Comput. **267**, 341–355 (2015)
20. Lovadina, C., Lyly, M., Stenberg, R.: A posteriori estimates for the Stokes eigenvalue problem. Numer. Methods Partial Differ. Equ. **25**(1), 244–257 (2008)

21. Luo, F., Lin, Q., Xie, H.: Computing the lower and upper bounds of Laplace eigenvalue problem: by combining conforming and nonconforming finite element methods. Sci. China Math. **55**(5), 1069–1082 (2012)
22. Mercier, B., Osborn, J., Rappaz, J., Raviart, P.: Eigenvalue approximation by mixed and hybrid methods. Math. Comput. **36**(154), 427–453 (1981)
23. Nakao, M.: A numerical verification method for the existence of weak solutions for nonlinear boundary value problems. J. Math. Anal. Appl. **164**, 489–507 (1992)
24. Nakao, M.T., Yamamoto, N., Watanabe, Y.: A posteriori and constructive a priori error bounds for finite element solutions of the Stokes equations. J. Comput. Appl. Math. **91**(1), 137–158 (1998)
25. Plum, M.: Explicit H^2 -estimates and pointwise bounds for solutions of second-order elliptic boundary value problems. J. Math. Anal. Appl. **165**, 36–61 (1992)
26. Rannacher, R., Turek, S.: Simple nonconforming quadrilateral Stokes element. Numer. Methods PDEs **8**, 97–111 (1992)
27. Takayasu, A., Liu, X., Oishi, S.: Verified computations to semilinear elliptic boundary value problems on arbitrary polygonal domains. NOLTA, IEICE, E96-N, No. 1, pp. 34–61 (2013)